SENSOR TASKING FOR MULTI-SENSOR SPACE OBJECT SURVEILLANCE

C. Frueh

Purdue University, School of Aeronautics and Astronautics, West Lafayette, IN 47907-2045, USA, Email: cfrueh@purdue.edu

ABSTRACT

Efficient sensor tasking is a crucial step in building up and maintaining a catalog of space objects at the highest possible orbit quality. With increased sensing capabilities, also the amount of objects that can be and are thought to be kept in the catalog is increasing. Realistic object numbers can easily reach over 100000 objects. It is crucial to note that for efficient collision avoidance and surveillance, individual information of those objects is sought rather than merely statistical information. Sensor resources are necessarily of a much smaller number compared to the number of objects. The object probability density function, and hence how good a catalog is, is influenced by the number of observations, the spacing and their quality. This makes sensor tasking a crucial step in order to ensure the best possible space object catalog. The best possible space object catalog can be defined as fulfilling a number of criteria. In the approach in this paper reformulates sensor tasking as an optimization problem. A cost function that is apt to the SSA tracking and cataloging problem is derived. The method is flexible enough to being able to incorporate multiple sensors with different observation schedules. The method can operate on a known a priori catalog of objects or be started on first principles. Computational feasible ways to evaluate the optimization are are shown and evaluated. The result shows a highly efficient sensor tasking scheme.

Keywords: LaTeX; ESA; macros.

1. INTRODUCTION

One of the aims of Space Situational Awareness (SSA) and a prerequisite for Space Traffic Management (STM) is the build-up and maintenance of an as complete and as comprehensive as possible information on each individual space object. The set of information on the objects is often referred to as a catalog; a catalog can include a plethora of information; a minimum is dynamical information, such as the state, position and velocity or equivalent.Only a minority of the human-made objects are active and of course communication is limited to the owner-operator; furthermore direct communication does not automatically guarantee a good determination of the satellite state probability density function. Information of uncooperative targets can be gained with active and passive ground based or space based sensors. The expected number of targets is in the order of 100'000 objects of interest [Pel16]. In comparison to this number, the number of sensors to collect independent information is relatively small. The large relative velocity differences between sensors and objects in different orbital regions prevent the simultaneous detection of very diverse objects, even if the field of view of the sensor would allow for it. The forces acting upon the object can only be modeled to a limited accuracy. This leads in combination with the non-linear nature of the space object orbits to an increasing position uncertainty. This makes re-observation of the objects necessary to keep custody.

Well designed sensor tasking is hence crucial. Traditionally, so-called surveys and follow-up observations are discriminated. Traditionally, survey and follow-up strategies have been developed for geosynchronous orbital regions [ASM$^+$, SHP99, Sch03, MSFB05, MSPB05]. Similar strategies have been adapted for the low Earth region for radar sensors [ELB11]. In recent research, these classical methods have been contrasted with other sensor tasking strategies. Fujimoto and Nafi [NF16] investigated different cost function models to evaluated different sensor tasking scenarios, based upon the traditional stripe scanning. Many publications however focus on either high level structures or do not give details on the merits that are actually gained, and are hence not or only limited operational applicable, e.g.[HHG$^+$16]. Some other strategies focusing on combining finite set statistics with sensor tasking [FHGS16] or machine learning [FSP16], or the use of genetic algorithms [HFS16].

In this paper, a new way of planning and conducting surveys is presented, in treating the sensor tasking and object coverage as an optimization problem via a weighted sky area approach in combination with diversification of the optimization scheme allowing for a very fast computation of a near optimal solution. This allows for a fast computation based on an a prior catalog, alternatively, the optimization can also be started based on first principles only. The method is flexible enough to

incorporate any number of optical sensors with different sensor characteristics. The paper is organized as the following: First the full optimization problem is introduced. In the second section, a computationally fast and feasible way of computing a near-optimal solution is shown. The paper concludes with simulations of two different sensors observing the geostationary ring with the aim to cover each object once or twice within one summer night. Their performances are compared. Preliminary research on this topic has been published in [Fru16], where one sensor was compared to a classical stripe-scanning sensor tasking, as developed in [ASM$^+$, SHP99, Sch03].

2. FORMULATION OF THE PROBLEM

2.1. Optimization Criteria

The optimization criteria that are sought to be maximized are:

1) initial detection
2) initial orbit determination of new objects
3) keeping custody/orbit improvement of known objects

The first principle is equivalent to maximizing the probability of detection in a twofold:

1.1) probability of detection, when the object is in the field of view (illumination etc.)

1.2) the number of objects observed simultaneously in the field of view per viewing direction

For the initial orbit determination The first item refers to getting the best possible signal to noise ratio (SNR) for the objects that are sought to be detected. The latter just means it is not very advantageous to observe regions of the sky which contain no objects (if known beforehand).

The second principle entails that observations have been collected in a manner, that a first orbit determination without a priori information is possible. First orbit determination methods include classical solutions to Lambert's problem, or the time-ordered equivalent using, Gauss or Lagrange method. The orbit improvement, the third principle, aims to collect observations, to update the probability density functions that are already known. Through the non-linear propagation in the presence of processing noise, the uncertainty grows over time. In order to keep an object in custody observation updates are needed to update the orbit with a smaller uncertainty again. The second and the third principle can be merged, if one views first orbit determination in a way that the single tracklet allows to determine a first orbit, with very large uncertainties, such as in an admissible regions approach [MGF$^+$09, TMFR09, MSC01].

2.2. Complete Formulation

Formulating the problem in the standard form leads to a the constrained optimization problem:

$$\max A = \sum_{g=1}^{l} \sum_{h=1}^{r_g} \sum_{f=1}^{m_g} \sum_{t_{g,f}=1}^{j_g} \big[\sum_{i=1}^{n} \mu_{\text{past}} \cdot p \cdot d + k \big]. \quad (1)$$

$$\begin{aligned} \alpha_{f,g} - \frac{1}{2}\text{FOV} - \alpha_i &\leq 0, & (2)\\ -\alpha_{f,g} - \frac{1}{2}\text{FOV} + \alpha_i &\leq 0, & (3)\\ \delta_{f,g} - \frac{1}{2}\text{FOV} - \delta_i &\leq 0, & (4)\\ -\delta_{f,g} - \frac{1}{2}\text{FOV} + \delta_i &\leq 0, & (5)\\ \mathbf{R} - \sigma &\leq 0. & (6) \end{aligned}$$

All function dependencies have been suppressed for a abbreviated more legible display. $A : \mathbb{R}^{k+4} \to \mathbb{R}$ being the cardinality of the weighted viewing direction areas, which is the quantity that is thought to be maximized. It is computed as the sum over all sensors l that can be employed at any time in the optimization interval. The second sum is over the r_g single time intervals for a given sensor g within the optimization interval of length $t_{\text{obs},g,h}$. A sensor might not be available during the entire observation interval, for example optical sensors during the day (although this could also be handled via the probability of detection), because of maintenance downtime, or time-slots that are pre-allocated to other task in a shared use instrument. The third sum is over all m_g viewing directions that are possible to be fit into the given observation interval for a given sensor. m_g is determined as $m_g = \text{int}(t_{\text{obs},g}/t_{\text{frame},g})$, with $t_{\text{frame}} = t_{\text{repos}} + j \cdot t_{\text{exp}} + (j-1) \cdot t_{\text{read}}$. $t_{\text{frames},g}$ is the time it takes the specific sensor to make a fixed number of frames j_g with exposure time t_{exp}, readout time t_{read} and repositioning time t_{repos}, for the last frame in a series, repositioning and readout can be done simultaneously. The optimization scheme is compartmentalized into the single time steps, $t_{f,g}$, that are corresponding to each of the j_g exposures. The time discretization may be different for each sensor, based on the fact that observations are started as soon as the sensor is available in continuous time. $\mu_{\text{past}} \in [0, 1]$ is the orbit quality function. It is a probability function that is applied as a weighting function, depending on the individual objects. If the objects are sought to be observed disregarding any prior history, $\mu_{\text{past}} = 1$. For all other cases, μ_{past} is a weight that rates, as of to when new observations are most benefiting to improve the orbital quality of the observed objects during the optimization interval. It is strictly periodic with the orbital period of the object. The orbit quality function is discussed in more detail in the next subsection.

$p(\alpha_i, \delta_i, \boldsymbol{o}, t_{g,f}) \in [0, 1]$ is the probability of detection of the single object of interest located at right

ascension $\alpha_{i,\mathrm{f}}$ and declination $\delta_{i,\mathrm{f}}$ at the time $t_{g,f}$. The probability of detection is not only dependent on the astrometric position of the objects, but also on other parameters, conflated under $\boldsymbol{o} \in \mathbb{R}^k$ including distance to the observer and the sun, location of the sun and object-dependent parameters, such as the object's size, shape, attitude, and surface reflection properties. In the chosen representation, the function $d(\alpha_{f,g}, \delta_{f,g}, \alpha_i, \delta_i, t_{g,f}) : \mathbb{R}^4 \rightarrow \mathbb{R}$ has been defined to represent the sensor to object association, for sensor g and object i at time $t_{g,f}$ for a given viewing direction of the sensor right ascension and declination, $\alpha_{f,g}, \delta_{f,g}$, respectively, at the same time. The association function is one when the boundary conditions (Eq. 12 to 16) are fulfilled and zero otherwise. Theoretically one could merge functions p and d into one function, defining that the probability of detection is zero when the object is not in the field of view (FOV) of the sensor, however for cleanness of representation and ease of understanding the more extensive definition has been selected, treating probability of detection as a weighting function for the association.

The constraints embed a twofold. For one, Eq. 12 to 15, the objects can only be observed if they are in the field of view (FOV) (d=1) at the time of observation $t_{g,f}$ for given objects and viewing directions. Currently, the location of the object $(\alpha_{i,\mathrm{f}}, \delta_{i,\mathrm{f}})$ is identified by the mean of its object probability density function (pdf) at that time. Secondly, Eq. 16 represents the re-observation constraint. The association is only valid ($d = 1$) when the object specific function $\sigma(\alpha_i, \dot{\alpha}_i, \delta_i, \dot{\delta}_i, \rho_i, \dot{\rho}_i, \nu, t_{g,f}) : \mathbb{R}^{6+q} \rightarrow \mathbb{R}^r$ is above or at a threshold $\mathbf{R} \in \mathbb{R}^r$. σ is a function of the full state of the object at minimum and potentially other parameters represented in ν or explicit time dependence. One interpretation of σ could be the object pdf covariance. This way, objects are actively sought to be observed when they experience a covariance above a certain threshold, and do not count towards A, when their covariance is small. This leads to holding objects in custody, when for example U is set to be half of the field of view in the project right ascension, declination direction. Voluntarily, the two orbit criteria have been chosen, threshold $\mathbf{R}$ and the orbit quality function μ_{past}. Theoretically, the two could be combined to avoid a cutoff threshold $\mathbf{R}$, however this comes at the huge disadvantage of disregarding the dynamical distinctions of the problem. Hence, it has been chosen to clearly separate the effects that are periodic with the orbital period from the secular effects in the optimization.

In the absence of already observed objects and their location (pdfs respectively) or other a priori knowledge, the first half of Eq.1 is zero. It will automatically populated as soon as objects have been observed and orbit determination has been performed. In order to be able to start a scenario without a prior information, or maintain a scenario not based upon single objects, the function $k(\alpha_{f,g}, \delta_{f,g}, t_{g,f}) : \mathbb{R}^k \rightarrow \mathbb{R}$ has been introduced. k can be understood as a multi-variate

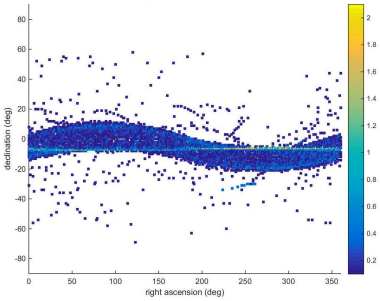

Figure 1: Binned TLE catalog object positions over July 12th observation night relative to the Zimmerwald (Switzerland) topocentric location.

weighting function that is projected in the observation plane of right ascension and declination. The potentially continuous function leads to a scalar value for each viewing direction $\alpha_{f,g}, \delta_{f,g}$ for a given sensor at a given time $t_{g,f}$. The pdf itself can be hence understood as mapping out probability in the physical surveillance space. A representation of k binned in right ascension and declination relative to an observer an be seen in Fig.1. Based on the TLE catalog, regions have assigned values between zero, no objects are likely to be present, to the maximum number of objects are present within the 24h period. Alternatively, k can be based upon regions of interest defined by a user or derived from astrodynamic principles from scratch for all objects or objects of interest. k has the advantage that it does not have to define single objects that are counted but simple values for given viewing directions. k can also be normalized to represent a probability measure.

When computing the optimization, either k or $p \cdot d$ or both can have assigned values. The advantage of the formulation given in Eq.1 to 16 is that no hard decisions need to be encoded, but the optimization itself balances the single objects, initial detection upon a priori information or first principles and keeping custody of the objects that have been already observed. The problem can be solved if it fulfills the convexity criteria both, in time, that is at every time step, and over time as the objects are not static. Although, the problem is solvable (at least for static objects), e.g. via branching methods, it is NP-hard, with object numbers of around $n \approx 1300$ (corresponding to the number of GEO objects currently in the TLE catalog) would take a long time to provide an exact solution. The pick of the viewing direction of the first frame even for a single sensor influences the viewing direction of **all** subsequent viewing directions. Solutions for the problem are along the lines of branch and bound algorithms, and sequential methods.

2.3. Discussion of the Orbit Quality Weighting Function

The orbit quality probability function is an periodic function. Based on past observations, not all observations

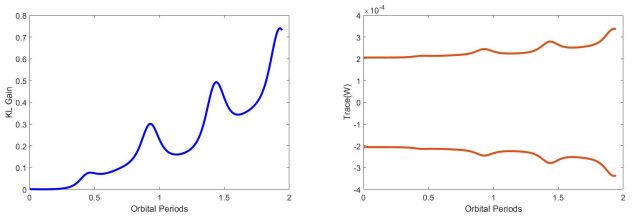

(a) KL information gain (b) Trace Information Covariance

Figure 2: Time history of (a) the Kullback-Leibler information gain and (b) of the trace of the innovation covariance.

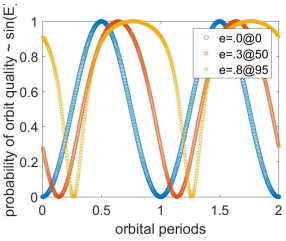

Figure 3: Probability of orbit quality for three different orbits with first observation at true anomalies of zero, 50, and 95 degrees and eccentricities of zero, 0.3, and 0.8.

along the orbit have the same impact on improving the orbit quality. There are several ways to evaluate how the orbit quality can be best improved. One way is to use observability as a measure, as shown in [FF17, FF16]. Alternatively, information measures have been evaluated [DJ11, CVS16, HFS16] based on the orbital probability density functions; often the Kullback-Leibler information gain is used:

$$G_{\mathrm{KL}} = \frac{1}{2}\log_{10}\frac{|\mathbf{P}^-|}{|\mathbf{P}^+|}, \tag{7}$$

$|\mathbf{P}^-|$ and $|\mathbf{P}^+|$ is the determinant of the covariance matrix prior and after a measurement update, respectively. The update is computed sampled from a predefined measurement uncertainty. The Kullback-Leibler information gain is displayed in Fig.2a. The same qualitative result can be achieved computing the information covariance without measurement updates, see Fig.2b:

$$\mathbf{W} = \mathbf{H}\mathbf{P}^-\mathbf{H}^T. \tag{8}$$

$\mathbf{H}$ is the measurement matrix. It has the advantage that no explicit update has to be computed; that means no sample needs to be drawn. It is simply the projection of the covariance in the measurement space. A simplified sinusoidal curve can be chosen of the eccentric anomaly E, to mimic the known uncertainty pattern in the measurement space. It is shown in Fig.11.

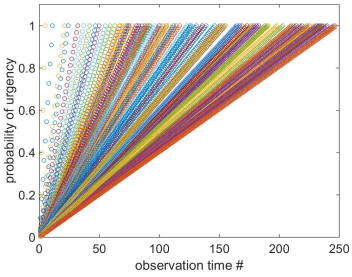

Figure 4: Diversification in time and over time for local optimization via the urgency probability function.

3. FAST NEAR OPTIMAL SOLUTION

In order to reduce the computational burden, the problem is reformulated, allowing for a near-optimal solution of the problem. Two simplifications have been made. The first one, is that not all viewing directions are allowed, but only fixed grid points in the right ascension, declination space can be visited. The grid is sized by the size of the field of view of the given sensor, such that all of the sky is covered without gaps. Although there is no physical reason fir this, it greatly reduces the load on the optimization problem. The second approximation that is made to avoid one of the sums of expression Eq. 1. Instead of optimizing for the exact observation times $t_{g,f}$, which are j_g time steps for each viewing direction, the mid-exposure time of the series is selected as the optimization criteria. This would be one time $m_g \rightarrow \tau_{g,f}$ for each observation direction f. A third simplification is to evaluate the expression at the local optimum instead of the global one. The local optimum however does not coincide with the global optimum, in general. This is only the case when no *conflicts*. Conflicts can be divided into two groups, in-time conflicts and over-time conflicts. In-time conflicts mean, that for the same time step, more than one viewing area has the same value. It is hence not immediately clear, which one to choose. More severely, however, are over-time conflicts. This means, that the overall at a time a viewing direction area might have a lower value, but at later times, selecting the lower value area will lead to a more optimal overall result. In order to counteract time conflicts, the so-called urgency function u has been added in the expression. he urgency function $u(t)$ is simply evaluating for how long an object is visible in the given optimization scenario and creating a function that linearly increases with the decrease of the remaining time at any given time step. A representation can be found in Fig.4. As a side effect, it also diversifies the values at the same time step and hence reduces in-time conflicts as well.

This leads in summary to the following, altered, computationally faster formulation of the optimization problem, described in Eq.1 that allows for evaluation via the local

optimum:

$$\max \tilde{A} = \sum_{g=1}^{l} \sum_{h=1}^{r_g} \sum_{f=1}^{m_g} \left[\left(\sum_{i=1}^{n} u \cdot \mu_{\text{past}} \cdot p \cdot d + k \right] \right. \quad (9)$$

$$\alpha_{f,g} = \{\alpha_1, \alpha_2, ..., \alpha_m\}, m \in \mathbb{N} \quad (10)$$

$$\delta_{f,g} = \{\delta_1, \delta_2, ..., \delta_m\}, m \in \mathbb{N} \quad (11)$$

$$\alpha_{f,g} - \frac{1}{2}\text{FOV} - \alpha_i \leq 0 \quad (12)$$

$$-\alpha_{f,g} - \frac{1}{2}\text{FOV} + \alpha_i \leq 0 \quad (13)$$

$$\delta_{f,g} - \frac{1}{2}\text{FOV} - \delta_i \leq 0 \quad (14)$$

$$-\delta_{f,g} - \frac{1}{2}\text{FOV} + \delta_i \leq 0 \quad (15)$$

$$\mathbf{R} - \sigma \leq 0 \quad (16)$$

Again, the function dependencies have been omitted in the above expressions for tidier representation.

4. SIMULATIONS FOR PROBABILITY OF DETECTION EQUAL ONE

Two different sensors are compared. According to the SMARTnet sensors of the German Aerospace Center (DLR), one sensor holding a 3.77 x 3.77 degrees FOV, denoted large FOV, or LFOV in the following, and one sensor holding a 0.6115 by 0.6115 degrees FOV has been modeled, denoted small FOV, or SFOV, respectively. The sensors have been chosen to be located in Zimmwald, Switzlerand. Ther sensor characteristics besides the field of view are chosen to be identical. Exposure time of eight seconds, readout time of seven seconds, repositioning within the stripe nine seconds and a repositioning to the beginning or the next stripe 30 seconds. Seven exposures per declination point are taken. Eight declination positions are chosen to cover the dispersion of the known objects in inclination. Whereas the LFOV telescope is a classical survey telescope, the SFOV has disadvantages in that respect. However, the SFOV allows for larger apertures, which gives a better probability of detection, in general. The common opinion is that the SFOV should not be used in survey; classical stripe scanning is not possible. In our scenario, we can still find a strategy for both sensors. Fort he sake of demonstration, probability of detection of one for all objects is assumed. As the underlying catalog the TLE catalog, provided by the USSTRATCOM is used, from the date July 12, 2016, observing from astronomical sunset to sunrise; comprising a short 360 minute observation night. The catalog has been filtered for near-gesynchronous objects with an altitude over 34'000 km. The grid for the viewing directions is finer for the SFOV and wider for the LFOV.

4.1. One Observation per Geosynchronous Mean Motion Object

In the first scenario one observation per GEO object is sought. Fig.5 shows the visible objects and the chosen viewing directions for both sensors (based on local horizon, sun set and rise times; earth shadow neglected). Based on the different FOV, the strategy is different for the two sensors. The optimization as shown above is

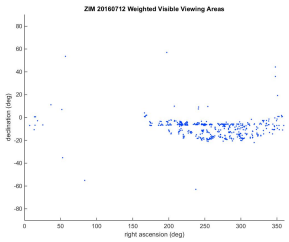

(a) all visible objects

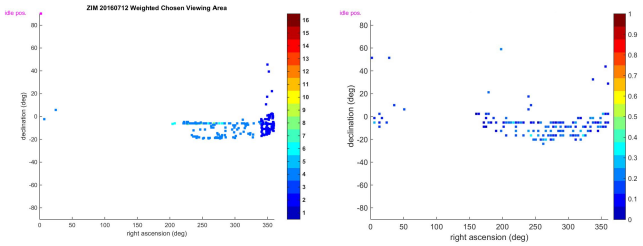

(b) SFOV (c) LFOV

Figure 5: (a) All near geosynchronous objects that are visible in at July 12, 2016 at the beginning of the observation scenario (based on the TLE catalog), chosen grid point viewing directions (b) SFOV and (c) LFOV by the optimization scheme.

based on the simple formulation taking the local optimum 9. For the validation of the performance, the exact scenario with the exact exposure times are use. In Fig.6 the detected objects are shown in turquoise and the undetected objects in dark blue for both sensors. The rates are shown in Fig.7. It shows that with the large FOV, all visible objects can be detected in the single night (assuming probability of detection equal to one). The small FOV, although a lot less suited us able to to observe a significant amount of the visible objects, over 30 percent.

4.2. Two Observations per Geosynchronous Mean Motion Object

In the second scenario two observations per GEO object is sought. Fig.8 shows the chosen viewing directions for both sensors (based on local horizon, sun set and rise times; earth shadow neglected). As the objective changed, for both sensors the strategy is altered significantly.

In Fig.9 the detected objects are shown in turquoise and

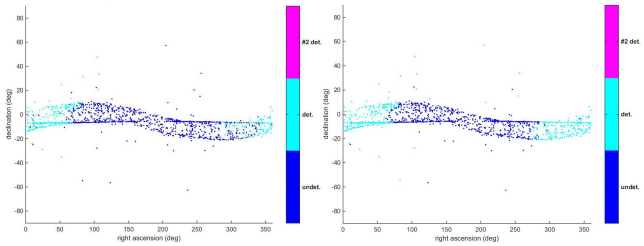

(a) SFOV (b) LFOV

Figure 6: July 12, 2016 detected (turquoise) and undetected objects (dark blue).

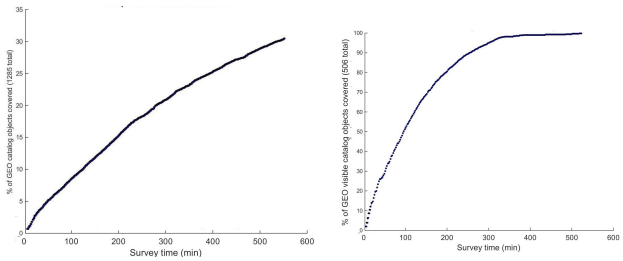

(a) SFOV (b) LFOV

Figure 7: July 12, 2016 detected object rate.

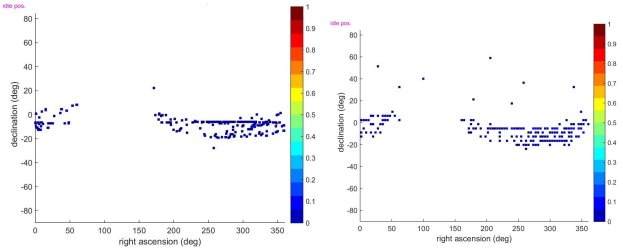

(a) SFOV (b) LFOV

Figure 8: July 12, 2016, chosen grid point viewing directions SFOV and LFOV optimized for two observations per object.

the undetected objects in dark blue for both sensors. The rates are shown in Fig.10. It shows that with the large FOV, all visible objects can be detected in the single night (assuming probability of detection equal to one). For the large field of view, almost 90 percent of the visible objects can actually be observed twice during the single summer observation night. Interestingly enough, the small FOV sensor is able to observe over 40 percent of the objects twice, which is actually a larger rate than the number of objects that have been observed once. The reason lies in the optimization scheme. In the first scenario, objects that have been already observed do not count any more, and are hence avoided. Here, it is a benefit to observe objects twice, so viewing directions that are able to observe more objects at once are observed twice, resulting in a higher rate in total. Fig.11 shows the spread in anomaly that has been achieved. The

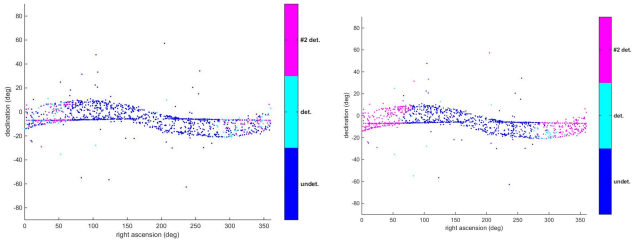

(a) SFOV (b) LFOV

Figure 9: July 12, 2016; objects detected once (turquoise), twice (magenta) and undetected objects (dark blue).

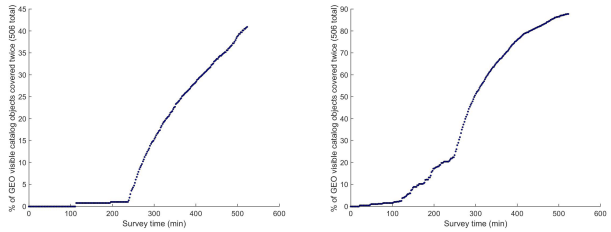

(a) SFOV (b) LFOV

Figure 10: July 12, 2016 rate of two observations per object.

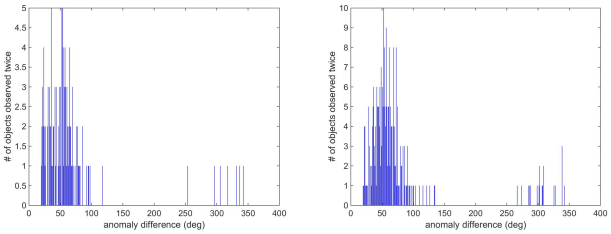

(a) SFOV (b) LFOV

Figure 11: July 12, anomaly differences between the two observation batches.

largest anomaly differences are achieved by the drifters. For the actual geostationary orbits, anomaly differences of on average around 50 degrees can be achieved within the same night.

5. CONCLUSIONS

The problem of efficiently cataloging all space objects has been reformulated as an optimization problem. In order to reduce the computational complexity, a grid based viewing direction formulation has been introduced at averaged times has been introduced. In introducing the urgency function, it has been made possible to to find a near-optimal solution to the optimization problem via local optimum evaluation. The very fast algorithm

produces excellent results for the sensor tasking of two different sensors, a large field of view sensor (LFOV) and a small field of view sensor (SFOV). The LFOV sensor has a field of view of 3.7 by 3.7 degrees, a classical survey telescope the SFOV sensor only has a FOV of 0.6115 by 0.6115 degrees. It used to be judged that the SFOV cannot perform surveys in an efficient manner.

In the simulations, using probability of detection of one at all times (neglecting earth shadow), the LFOV sensor operating by itself, was able to observe all visible objects once per night during a 360 minute observation night. Running the night again, it was able to observe over 90 percent of the objects twice with a good anomaly spread of the observations. The SFOV sensor still reached a coverage of over 30 percent for one obseravtion per object. For two observations per object, the same scenario could even reach a coverage of over 40 percent of the objects in the single observation night.

Future work includes the extension of the framework to derive survey fields based on first principles independent of the two line element data sets and the inclusion of full object probability density functions and the operation of the sensors in a synchronous scenario.

ACKNOWLEDGMENTS

Many thanks goes the SSA Group, GSOC DLR Oberpfaffenhofen for the support of this work in 2016. Many thanks for fruitful and tough discussions is due to Dr Oliver Montenbruck. Many thanks also to Dr Kyle DeMars for fruitful discussions concerning information gain. Thanks also to Martin Weigel for providing many useful comments on the manuscript.

REFERENCES

ASM+. J. Africano, T. Schildknecht, M. Matney, P. Kervin, E. Stansbery, and W. Flury. A Geosynchronous Orbit Search Strategy, Space Debris. *Space Debris*, 10:357–369.

CVS16. E. Cordelli, A. Vananti, and T. Schildknecht. Covariance study to evaluate the influence of optical follow-up strategies on estimated orbital parameters. *Acta Astronautica*, 122:76 – 89, 2016.

DJ11. Kyle J. DeMars and Moriba K. Jah. Evaluation of the information content of observations with application to sensor management for orbit determination. volume 142 of *Advances in the Astronautical Sciences*, pages 3169–3188, 2011.

ELB11. J. Ender, L. Leushacke, and A. Brenner. Radar techniques for space situational awareness. In *IEEE Radar Symposium (IRS), 2011 Proceedings International*, 2011.

FF16. A. Friedman and C. Frueh. Observability analysis applied to artificial near-earth objects with noise. Space Flight Mechanics Meeting, San Antonio, TX, February 2016. 27th AAS/AIAA Space Flight Mechanics Meeting. AAS 17-237.

FF17. A. Friedman and C. Frueh. Determining Debris Characteristics From Observability Analysis of Artificial Near-Earth Objects. In *Proceedings of the Seventh European Conference on Space Debris, ESOC, Darmstadt, Germany, 18-21 Aprill 2017*, 2017.

FHGS16. J. Ferreira, I. Hussein, J. Gerber, and R. Sivilli. Optimal SSN Tasking to Enhance Real-time Space Situational Awareness. In *Proceedings of the 2009 AMOS Technical Conference, 20-23 September 2016, Maui, Hawaii, USA*, 2016.

Fru16. C. Frueh. Realistic Sensor Tasking Strategies. In *Advanced Maui Optical and Space Surveillance Technologies Conference (AMOS)*, September 2016.

FSP16. C. Frueh, T. Schildknecht, and M. Ploner. . In *Proceedings of the 2009 AMOS Technical Conference, 20-23 September 2016, Maui, Hawaii, USA*, 2016.

HFS16. A. Hinze, H. Fiedler, and T. Schildknecht. Optimal Scheduling for Geosynchronous Space Object Follow-up Observations Using a Genetic Algorithm. In *Advanced Maui Optical and Space Surveillance Technologies Conference (AMOS)*, September 2016.

HHG+16. A. Herz, E. Herz, D. Georger, P. Axelrad, and B. Jones. Utilizing Novel Non-Traditional Sensor Tasking Approaches to Enhance the Space Situational Awareness Picture Maintained by the Space Surveillance Network. In *Proceedings of the 2009 AMOS Technical Conference, 20-23 September 2016, Maui, Hawaii, USA*, 2016.

MGF+09. A. Milani, G.F. Gronchi, D. Farnocchia, G. Tommei, and L. Dimare. Optimization of Space Surveillance Resources by Innovative Preliminary Orbit Methods. In *Proceedings of the Fifth European Conference on Space Debris, ESOC, Darmstadt, Germany, 30 March-2 April 2009*, 2009.

MSC01. A. Milani, M.E. Sansaturio, and S.R. Chesley. The Asteroid Identification Problem IV: Attributions. *Icarus*, 151:150 – 159, 2001.

MSFB05. R. Musci, T. Schildknecht, T. Flohrer, and G. Beutler. Concept for a Catalogue of Space Debris in GEO. In *Proceedings of the Fourth European Conference on Space Debris, pp. 601-606, ESOC, Darmstadt, Germany, 18-20 April 2005*, 2005.

MSPB05. R. Musci, T. Schildknecht, M. Ploner, and G. Beutler. Orbit Improvement for GTO Objects

Using Follow-up Obervations. *Advances in Space Research*, 35(7):1236–1242, 2005.

NF16. A. Nafi and K. Fujimoto. A unified approach for optical survey strategy design of resident space objects. In *AAS/AIAA Astrodynamics Specialist Conference*, Sep 2016.

Pel16. J. Pelton. *Tracking of Orbital Debris and Avoidance of Satellite Collisions, Handbook of Satellite Applications*. 2016. Springer, New York.

Sch03. T. Schildknecht. *The Search for Space Debris Objects in High-Altitude Orbits*. Astronomical Institute, University of Bern, 2003. Habilitation treatise.

SHP99. T. Schildknecht, U. Hugentobler, and M. Ploner. Optical Surveys of Space Debris in GEO. *Advances in Space Research*, 62(1):45 – 54, 1999.

TMFR09. G. Tommei, A. Milani, D. Farnocchia, and A. Rossi. Correlation of Space Debris Observations by the Virtual Debris Algorithm. In *Proceedings of the Fifth European Conference on Space Debris, ESOC, Darmstadt, Germany, 30 March-2 April 2009*, 2009.